Quantitative Space-bandwidth product comparison of different digital holographic setups

Daniel Claus[1,*], Daciana Iliescu[2] and Peter Bryanston-Cross[2]
[1] *Kroto Research Institute, University of Sheffield,S3 7HQ, Sheffield, UK*
[2] *School of Engineering, University of Warwick, CV4 7AL, Coventry, UK*
[*] *Corresponding author: d.claus@sheffield.ac.uk*

The Space-Bandwidth Product (SBP) is a measure for the information capacity an optical system possesses. The two information processing steps in digital holography, recording and reconstruction, are analysed with respect to the SBP. The recording setup for a Fresnel hologram, Fourier hologram and Image-plane hologram, which represent the most commonly used setup configurations in digital holography, are investigated. For the recording process, the required SBP to ensure the recording of the entire object information is calculated. This is accomplished by analysing the recorded interference pattern in the hologram plane. The paraxial diffraction model is used in order to simulate the light propagation from the object to hologram-plane. The SBP in the reconstruction process is represented by the product of the reconstructed field of view and spatial frequency bandwidth. The outcome of this analysis results in a space-bandwidth product optimised digital holographic setup.
OCIS codes: 090.1995, 050.5082, 070.0070, 350.5730, 050.1940, 070.7345

1. Introduction

This paper concentrates on the evaluation of the imaging performance of different digital holographic setup configurations. Conventionally, the modulation transfer function (MTF) is used to describe the imaging performance of optical systems. However, the MTF only takes into account how various spatial frequencies are affected by their passage through the optical system. A more meaningful parameter is the Space-Bandwidth Product (SBP), which additionally takes into account the field of view an optical system can cover. In this manner a comparison of the imaging performance for various optical systems such as a microscope objective or a telescope can be achieved.

In this paper the SBP is evaluated comparatively for the recording and reconstruction processes of three most commonly used digital holographic setups, which is based on a planar two-dimensional object. The outcome of this study can be used to configure a digital holographic system which has the highest information density and hence enables the transfer of the highest amount of data from the object to the reconstructed hologram.

An in depth study of the SBP in digital holography was conducted by Lohmann [1] and Xu et al [2]. Lohmann [1] studied the three holographic setup configurations with respect to their SBP in the recording process using the Wigner distribution function. His investigation of Fourier holograms was based on a lens, which converts the reference and object point source into plane waves and was done for an off-axis arrangement. On the other hand the studies described in [2] are only consideres Fresnel holograms in in-line and off-axis configurations.

Our investigation differs from that in [1] and [2] by modeling the propagation to the recording plane using the paraxial wave-propagation model, as discussed in [3]. The recorded interference pattern is analysed to reveal the phase and space transformation. This may be a less elegant way than proposed in [1] to obtain the required SBP in the recording process. However, important setup parameters defining the SBP in the reconstruction process can be derived with respect to the sampling condition (Nyquist criterion). Moreover, the proposed modelling of the propagation of light results in the full description of the phase terms involved. This knowledge can be used to recover only the object phase in the reconstruction process by suppressing other phase terms which do not contribute to the object phase.

The SBP is the physical quantity which describes the information density of an optical system. Without loss of generality only one dimension is considered for this and further explanations. Thus, the SBP of an object, given by the product of its size X and its spatial frequency bandwidth $\Delta\nu$, which can be expressed as:

$$SBP = X\Delta\nu \tag{1}$$

An important property is that the area covered by the SBP in the space frequency domain is independent of the transformation applied to it. To simplify the mathematical description and transformations applied to the SBP it is assumed that the infinitely defined spatial frequency of the signal has significant values within a finite, rectangular region only, as seen in Fig. 1(a). A Fresnel-transformation applied to the original SBP results in a shift of the spatial coordinate (Fig. 1(b)). The original SBP is rotated by 90° when a Fourier-transformation is applied to it (Fig. 1(c)). A shift in the spatial frequency coordinate is introduced by the passage of light through a lens or lens-system, see Fig. 1(d).

Our analysis assumes that the object under investigation is finite, band-limited and centred on the optical axis. Thus the maximum and minimum object extent in the x direction x_{max} and $-x_{max}$ are of the same magnitude, $X/2$, but opposite sign. Likewise, the frequency bandwidth $\Delta\nu$ of the object extends between the (+) and (-) limits of its highest spatial frequency ν_{x_max}, and it is represented by the inverse of the smallest resolvable object detail δ, as shown in Eq. 2.

$$\Delta\nu = 2\nu_{x\_max} = \frac{1}{\delta} \tag{2}$$

To distinguish between different planes, the nomenclature changes to include single quotes ($'$) for all parameters in the hologram plane and double quotes ($''$) for all parameters in the reconstruction plane (see Fig. 2).

2. Required SBP$'$ of The Recording Sensor

This section discusses how efficiently the sensor's SBP is used with respect to the optical arrangement. In order to ensure no loss of object-information, the SBP' for the recording sensor should be larger than the SBP of the object. Moreover, the minimum recording distance, which determines the obtained field of view (FOV) and the spatial frequency bandwidth, thus the SBP'' in the reconstruction process, should be set so that the interference pattern is not under-sampled (Nyquist criterion).

Let us consider the propagation of light from the object-plane to the hologram-plane. With the benefit of reducing the mathematical effort and without loss of generality, the spherical wavefront can be approximated by a parabolic wavefront:

$$u'(x') = \frac{\exp(ikd)}{i\lambda\, d} \int_{-\infty}^{\infty} u(x) \exp\left[\frac{i\pi}{\lambda\, d}(x'-x)^2\right] \mathrm{d}x \tag{3}$$

Where $u'(x')$ is the complex amplitude in the hologram plane, $u(x)$ is the complex amplitude in the object plane, $k = \frac{\lambda}{d}$ is the wave number, λ is the wavelength and d is the distance between object and hologram.

A. *Fresnel hologram*

A Fresnel hologram is recorded when a plane reference wave interferes with the spherical object wave, see Fig. 3. To obtain the largest spatial frequency for the recorded interference pattern in the hologram plane, the point x_o in the object-plane should be located at $-x_{max}$. For a real object, which can be modelled as a superposition of sinusoidal gratings with different frequencies, the largest resolvable grating frequency ν_o is determined by the size of the sensor X' according to Abbe's criterion. We can simplify the grating to a double slit, as shown in Fig. 4, which corresponds to two point sources A_{o1} and A_{o2}, located in close proximity to x_o and separated by:

$$x_{o2} - x_{o1} = 2\delta = \frac{1}{\nu_o} \tag{4}$$

By ignoring the constant phase term $\left(\frac{\exp(ikd)}{i\lambda\, d}\right)$ in Eq. 3 the paraxial propagation of light for each of the two point sources from the object-plane to the hologram-plane can be described as:

$$u'_{oj}(x') = A_{oj} \exp\left[\frac{i\pi}{\lambda d}\left(x' - x_{oj}\right)^2\right], \text{ where } j = 1, 2 \tag{5}$$

The intensity of the resulting interference pattern from both point sources, ignoring a further constant phase term $\left(x_{o1}^2 - x_{o2}^2\right)$, becomes:

$$\begin{aligned} I &= \left|u'_{o1}(x') + u'_{o2}(x')\right|^2 = \left[u'_{o1}(x') + u'_{o2}(x')\right] \cdot \left[u'_{o1}(x')^* + u'_{o2}(x')^*\right] \\ &= A_{o1}^2 + A_{o2}^2 + 2A_{o1}A_{o2} \cos\left[\frac{2\pi}{\lambda d}\left(x_{o2} - x_{o1}\right) x'\right] \end{aligned} \tag{6}$$

According to [1], [4] and [5] the spatial frequency bandwidth remains invariant under propagation from the object-plane to the hologram-plane. Therefore ν_0 in the object-plane matches ν'_o in the hologram-plane, allowing the substitution of $\frac{2\pi}{\lambda d}\left(x_{02} - x_{01}\right)$ with $2\pi\nu_o$ in Eq. 6:

$$I = A_{o1}^2 + A_{o2}^2 + 2A_{o1}A_{o2} \cos\left(2\pi\nu_o x'\right) \tag{7}$$

The interference of both propagating point sources at x_{o1} and x_{o2} results in a linear phase difference (phase tilt) according to Eq. 6. Between both propagating waves no parabolic phase difference exists, since both possess the same curvature. The two point sources generate a distorted spherical wave, see Fig. 4 (dashed line), with the object information stored in the wavefront distortion.

The phase of the parabolic object wave is visualized when the object wave interferes with a reference wave of different wavefront curvature. The propagating object wave can therefore be described as:

$$u'_o(x') = A_o \exp\left(i2\pi\nu_o x'\right) \exp\left[\frac{i\pi}{\lambda d}\left(x' - x_o\right)^2\right] \tag{8}$$

At the hologram-plane u'(x') the object wave interferes with a plane reference wave, as shown in Fig. 3. The plane reference wave can be described as:

$$u'_r(x') = A_r \exp\left(-i2\pi\nu_r x'\right) \tag{9}$$

where ν_r corresponds to the frequency of the reference wave. The interference pattern obtained can be described as:

$$I(x') = A_o A_o^* + A_r A_r^* + 2A_o A_r \cos\left[2\pi x'\left(\nu_o + \nu_r\right) + \frac{\pi}{\lambda d}\left(x' - x_o\right)^2\right] \tag{10}$$

The parabolic phase terms $\frac{\pi}{\lambda d}\left(x' - x_o\right)^2$ in Eq. 10 can be interpreted as a Fresnel lens with focal length $f = -d$. This parabolic phase term causes a spatial localization of the object wave in the hologram-plane.

It does not contribute to any additional object information and is therefore not taken into account for the spatial frequency consideration. However, the reference wave frequency in conjunction with this parabolic phase term can be used to calculated the minimum recording distance with respect to the Nyquist criterion, which will be used at a later stage to obtain the SBP'' in the reconstruction process.

On the other hand the coordinate transformation from the object-plane to the hologram-plane is obtained from the geometric relations shown in Fig. 5 as follows:

$$x' = x_o + \lambda d\nu_o \tag{11}$$

In-line Setup

For an in-line setup, $\nu_r = 0$, the spatial frequency recorded is ν_o. Hence the transformation of the spatial and frequency coordinates is:

$$(x_o, \nu_o) \rightarrow (x'_o, \nu'_o) = (x_o + \lambda d\nu_o, \nu_o) \tag{12}$$

$$\rightarrow (X', \Delta\nu') = (X + \lambda d\Delta\nu, \Delta\nu) \tag{13}$$

The required SBP' for an in-line Fresnel hologram can be obtained by multiplication of the space and frequency coordinates shown in Eq. 13:

$$\boxed{SBP'_{in-line} = X\Delta\nu + \lambda d\Delta\nu^2 = SBP + N_F^{-1}} \tag{14}$$

where N_F is the Fresnel number, described by the term $\lambda d\Delta\nu^2$ ([6]).

It was assumed that the complex object wave is already accessible when recording a single hologram only. However in practice this in not the case. The twin image, image and DC term overlap one another as shown in Fig. 6(b). The DC term results from the two autocorrelation terms of object wave ($A_o A_o^*$) and reference wave ($A_r A_r^*$), represented in Eq. 10. In addition to the overlap the DC term imposes another disturbing effect in the reconstruction. Due to the DC's terms large intensity the image is hardly visible in the reconstruction. The DC term therefore needs to be suppressed by various techniques such as subtracting the mean value or other procedures (see [7]). However, not only the DC-term but also the twin image disturbs the reconstruction in case an in-line setup has been used. In order to suppress the twin image phase stepping is generally applied for an in-line recording setup of short recording distance (see [8]). The number of additional holograms required for the phase stepping algorithm, typically three or more, needs to be multiplied by the magnitude of required SBP', shown in Eq. 14. Hence, the required SBP' to obtain a complex object wave utilizing a three bucket phase stepping algorithm, as discussed in [9], is six times larger than the object's SBP.

Off-axis Setup

Another way to suppress the overlap of image, twin image and DC-term in the reconstruction is the application of an off-axis setup, in which the reference wave and object wave interfere at a required angle α (see Fig. 3). Thus a spatial carrier frequency ν_r is superimposed with the object information. The recorded intensity contains three spatial frequency components (DC-term, image and twin-image), which can be separated in the Fourier domain. Hence the corresponding space-frequency-coordinate transformation are:

$$\begin{aligned}(x_o, \nu_o) &\rightarrow (x'_o, \nu'_o) = (x_o + \lambda d\nu_o, [-(\nu_o + \nu_r), (\nu_o + \nu_r)]) \\ &\rightarrow (X', \Delta\nu') = (X + \lambda d\Delta\nu, \Delta\nu + 2\nu_r)\end{aligned} \tag{15}$$

In this case the SBP$'$ becomes:

$$SBP'_{off-axis} = (X + \lambda d\Delta\nu)(\Delta\nu + 2\nu_r) \tag{16}$$

The SBP' for the off-axis arrangement is shown on Fig. 6(c). The main advantage of an off-axis setup is the ability to suppress the twin-image and the DC-term by solely recording a single hologram and filtering those terms in the Fourier domain (with the angle α carefully chosen to enable the separation). In the reconstructed hologram the autocorrelation of the reference wave matches the sensor size X', whereas the autocorrelation of the object wave expands over twice the object-size. In order to avoid an overlap between the DC terms, image (X'')[1] and twin-image in the reconstructed hologram ν_r needs to be:

$$\nu_r \geq \frac{3X}{\lambda d} = \frac{3}{2}\Delta\nu \tag{17}$$

The required reference wave carrier frequency to enable the separation and suppression of reconstruction terms is also graphically represented in the space frequency domain in Fig. 6(c). Digital holography enables the suppression of the DC term prior to the reconstruction, which results in a more efficient usage of the sensor's SBP. The introduction of DC term suppression techniques is furthermore encouraged by the fact that the spatial resolution of digital sensors (typically 200 lp/mm) is limited in comparison with that of holographic plates used in optical holography (3000 lp/mm). Therefore, the endeavour in digital holography is not to waste more spatial resolution than is needed for recording. The required reference wave carrier frequency for a DC term suppressed hologram is:

$$\nu_r \geq \frac{X}{\lambda d} = \frac{1}{2}\Delta\nu \tag{18}$$

Eq. 18 is then inserted into Eq. 16:

$$\boxed{SBP'_{off-axis} = 2\left(SBP + N_F^{-1}\right)} \tag{19}$$

In conclusion, the off-axis configuration requires the sensor's SBP' to be four times larger without DC term suppression (Fig. 6(c)) or two times larger with DC term suppression (Fig. 6(d)) than for the in-line configuration (Fig. 6(b)).

B. Fourier hologram

Two types of Fourier holograms exist based on lens system or a lensless setup. In both cases compensation for the curvature of the object wave, due to the propagation of light to the hologram plane, is achieved. For a lensless Fourier hologram the curvature of the object wave is compensated by using a spherical reference wave of equal curvature. Lens based Fourier holograms employ a convergent lens, with the hologram placed at the focal distance f, in order to compensate the object's wave curvature. A plane reference wave then interferes with the lens projected object wave. Lens based Fourier holograms and their influence on the SBP has been discussed in [1]. Under the assumption of an ideal lens (infinite extent of lens diameter and no wave aberrations) both systems result in the same required SBP'. Due to this similarity the SBP' derivation discussed here will consider only the lensless Fourier hologram case.

The complex reference wave can be described as:

$$u'_r(x') = A_r \exp\left[\frac{i\pi}{\lambda d_r}\left(x' - x_r\right)^2\right] \tag{20}$$

The recorded spatial carrier frequency depends on the lateral position of reference wave point source and object point. The largest spatial carrier frequency is obtained from the interference of the reference wave with an object point-source, described by Eq. 8, which is located at the furthest distance from the reference wave point source, see Fig. 7.

[1] X'' matches with the object-size X and can hence be replaced by it

The reference point source distance d_r and the object point source distance d are matched ($d_r = d$). The intensity pattern recorded can then be described as:

$$I(x') = A_r^2 + A_o^2 + 2A_oA_r \cos\left[\frac{\pi}{\lambda d}E\right], \text{ where } E = 2x'\nu_o\lambda d + (x' - x_o)^2 - (x' - x_r)^2 \tag{21}$$

The focus is now set on solving E. The second and third term in E are responsible for the reference frequency. From Fig. 7 follows that $x_r = x_{max}$ and $x_o = -x_{max}$, which results in:

$$(x' - x_o)^2 - (x' - x_r)^2 = -2x'x_o + x_o^2 + 2x'x_r - x_r^2 = 4x'x_{max} \tag{22}$$

From the two similar triangles (highlighted in red in Fig. 7) the following expression can be derived:

$$x_{max} = \frac{\lambda d}{2}\nu_r \tag{23}$$

Eq. 21 can be rewritten by substituting x_{max} in Eq. 22 with Eq. 23:

$$I(x') = A_r^2 + A_o^2 + 2A_oA_r \cos\left[2\pi x'\left(\nu_o + \nu_r\right)\right] \tag{24}$$

The appearance of the spherical phase factor inherent to the recording of Fresnel holograms is suppressed when recording a Fourier hologram. This is due to the application of spherical reference wave whose curvature is adapted to the object wave. This results in a *non* localized space-coordinate transformation $x' = \lambda d\nu_o$, meaning that the object information is homogenously distributed over the entire hologram.

In-line Setup

The transformation from the object to the hologram plane for an in-line configuration ($\nu_r = 0$) is:

$$\begin{aligned}(x_o, \nu_o) &\rightarrow (x'_o, \nu'_o) = (\lambda d\nu_o, \nu_o) \\ &\rightarrow (X', \Delta\nu') = (\lambda d\Delta\nu, \Delta\nu)\end{aligned} \tag{25}$$

The resulting required $SBP'_{in-line}$ is:

$$\boxed{SBP'_{in-line} = \lambda d\Delta\nu \cdot \Delta\nu = N_F^{-1}} \tag{26}$$

This again is based on the assumption that the complex object wave is already accessible when recording a single hologram only. The recording of additional holograms to access the phase data unambiguously needs to be accounted for, as described in the previous section (Fresnel hologram).

Off-axis Setup

In order to efficiently use the sensor's SBP' in the off-axis configuration DC term suppression techniques are applied, as discussed in [8] and [10]. The image and twin image can then be separated by locating the reference wave adjacent to the object-point which is at the furthest distance from the optical axis. The space frequency transformation can hence be described as:

$$\begin{aligned}&(x_o, \nu_o) \rightarrow (x'_o, \nu'_o) = (\lambda d\nu_o, [-(\nu_o + \nu_r), (\nu_o + \nu_r)]) \\ &\rightarrow (X', \Delta\nu') = (\lambda d\Delta\nu, \Delta\nu + 2\nu_r)\end{aligned} \tag{27}$$

Taking into account Eqs. 18 and 23, the required SBP' for an off-axis Fourier hologram becomes:

$$\boxed{SBP'_{off-axis} = = (\lambda d\Delta\nu)\, 2\Delta\nu = 2N_F^{-1}} \tag{28}$$

The required SBP' in the off-axis configuration is twice as large as in the in-line configuration. Moreover, SBP' in comparison with Fresnel holograms is smaller. A Fourier hologram introduces a rotation of space and frequency coordinates whereas the Fresnel hologram introduces a shear in the space coordinate, which results in an increase of the required SBP'. This is graphically shown in the space frequency domain by comparing Fig. 6 (Fresnel hologram) and Fig. 8 (Fourier hologram).

C. Image-plane hologram

The object is imaged onto the sensor with a lens or a lens-system as shown in Fig. 9. The recording of the real image of the object instead of the object itself can have some advantages ([11]), such as the possibility to position the projected image of the object when recording the hologram. Image-plane holograms are often used when the object is three dimensional but not very deep in the third dimension [3], allowing increased lateral resolution in the sub-micrometer range, e.g. in digital holographic microscopy. The viewing angle and the highest recordable spatial frequency is restricted by the numerical aperture (NA) of the imaging lens. For previous investigations of lens-less digital holographic setups only a single point in the object-plane has been considered. However, the single point source model can be no longer applied, since the result depends on the position of the point source in the object-plane u(x). Thus we need to consider the integral over all object points. The mathematical derivation shown in the following corresponds closely to the imaging equations discussed by [3] and [12]. At first, the light propagates in free space from the object to the first lens surface $u_{L1}(\tilde{x})$. This can be expressed as a *convolution* between the light distribution in the object-plane and the impulse response of the free space propagation and it is manifested by a *shear in the spatial domain* (as seen when recording a Fresnel hologram, see Fig. 1(b)).

At the first lens plane $u_{L1}(\tilde{x})$ a diverging spherical wave originating from the object plane can be registered.

$$u_{L1}(\tilde{x}) = \int_{-\infty}^{\infty} u(x) \exp\left[i\pi \frac{(x-\tilde{x})^2}{\lambda d_1}\right] \mathrm{d}x \tag{29}$$

From $u_{L1}(\tilde{x})$ light passes through the lens to arrive at the second lens surface $u_{L2}(\tilde{x})$. This is expressed by a *multiplication* between the incident wave-field and a phase term representing the curvature of the lens, resulting in a *shear in the frequency domain* (Fig 1(d)). Assuming the thin lens model, matched back focal length f and front focal length f', the following expression can be derived in the paraxial region:

$$u_{L2}(\tilde{x}) = u_{L1}(\tilde{x}) \exp\left(\frac{-i\pi\tilde{x}^2}{\lambda f}\right) \tag{30}$$

From the second lens surface light propagates to the hologram-plane $u'(x')$.

$$u'(x') = \int_{-\infty}^{\infty} u_{L2}(\tilde{x}) \exp\left[\frac{i\pi\,(\tilde{x}-x')^2}{\lambda d_2}\right] \mathrm{d}\tilde{x} \tag{31}$$

Substituting Eq. 29 and Eq. 30 in Eq. 31 results in:

$$\begin{aligned} u'(x') &= \int_{-\infty}^{\infty}\int_{-\infty}^{\infty} u(x) \exp\left[\frac{i\pi}{\lambda}\left\{\frac{(x-\tilde{x})^2}{d_1} - \frac{\tilde{x}^2}{f} + \frac{(\tilde{x}-x')^2}{d_2}\right\}\right] \mathrm{d}x\mathrm{d}\tilde{x} \\ &= \int_{-\infty}^{\infty}\int_{-\infty}^{\infty} u(x) \exp\left[\frac{i\pi}{\lambda}\left\{\tilde{x}^2\left(\frac{1}{d_2} - \frac{1}{f} + \frac{1}{d_1}\right) - 2\tilde{x}\left(\frac{x}{d_1} + \frac{x'}{d_2}\right)\right.\right. \\ &\quad \left.\left. + \frac{x^2}{d_1} + \frac{x'^2}{d_2}\right\}\right] \mathrm{d}x\mathrm{d}\tilde{x} \end{aligned} \tag{32}$$

An in focus image needs to satisfy the lens formula $\frac{1}{f} = \frac{1}{d_1} + \frac{1}{d_2}$, therefore the phase term $\left(\frac{1}{d_2} - \frac{1}{f} + \frac{1}{d_1}\right)$ in {...} should consequently become zero. Assuming that all conditions are met as explained in [13] to permit

the change of integration order, Eq. 32 becomes:

$$\begin{aligned} u'(x') = &\exp\left(\frac{i\pi x'^2}{\lambda d_2}\right) \int_{-\infty}^{\infty} u(x) \exp\left(\frac{i\pi x^2}{\lambda d_1}\right) \\ &\int_{-\infty}^{\infty} \exp\left[\frac{-2i\pi\tilde{x}}{\lambda}\left(\frac{x}{d_1}+\frac{x'}{d_2}\right)\right] \mathrm{d}\tilde{x}\mathrm{d}x \end{aligned} \tag{33}$$

Thus we can solve the integral of $\mathrm{d}\tilde{x}$ by applying a Fourier-transformation with the angular frequency $\hat{\omega} = \frac{x+\frac{x'd_1}{d_2}}{\lambda d_1}$.

$$u'(x') = \exp\left(\frac{i\pi x'^2}{\lambda d_2}\right) \int_{-\infty}^{\infty} u(x) \exp\left(\frac{i\pi x^2}{\lambda d_1}\right) \delta\left(\hat{\omega}\right) \tag{34}$$

Taking into account the scaling ($\delta(ax) = \frac{\delta(x)}{|a|}$) and shifting ($\int_{-\infty}^{\infty} f(x)\delta(x-a)\mathrm{d}x = f(a)$) properties of the δ-function ([14]), the integral in Eq. 33 can be solved as:

$$u'(x') = |\lambda d_1| u\left(-x'\frac{d_1}{d_2}\right) \exp\left[\frac{i\pi x'^2}{\lambda}\left(\frac{1}{d_2}+\frac{d_1}{d_2^2}\right)\right] \tag{35}$$

The factor $\left(\frac{d2}{d1}\right)$ in the argument of u denotes the magnification M of the optical system. The minus sign indicates an inverted image. The magnification M can also be defined by the object and image coordinates.

$$M = \frac{d_2}{d_1} = \frac{x'}{x} = \frac{d_2 - f}{f} \tag{36}$$

Ignoring the constant factor $|\lambda d_1|$, Eq. 35 can be described by M:

$$\begin{aligned} u'(x') &= u\left(-\frac{x'}{M}\right) \exp\left[\frac{i\pi x'^2}{\lambda d_2}\left(1+\frac{1}{M}\right)\right] \\ &= u\left(-\frac{x'}{M}\right) \exp\left(\frac{i\pi x'^2}{\lambda d_2}\right) \exp\left(\frac{i\pi x^2}{\lambda d_1}\right) \end{aligned} \tag{37}$$

If one is only interested in the intensity Eq. 37 already satisfies the condition to obtain an in-focus point in the image-plane. The complex exponential terms only affect the phase. If not only the intensity but also the phase is important the two parabolic phase terms in Eq. 37 need to be taken into account.

$$\exp\left(\frac{i\pi}{\lambda}\frac{x^2}{d_1}\right) \qquad \text{and} \qquad \exp\left(\frac{i\pi}{\lambda}\frac{x'^2}{d_2}\right)$$

The quadratic phase factor with respect to the x'-coordinate can be suppressed interferometrically by adapting the curvature of the reference wave to the curvature of the parabolic phase term. The quadratic phase term with respect to the x-coordinate can be neglected according to [3] if:

i. The object is on a spherical surface centered on the optical axis with a radius equal to d_1.

ii. The object is illuminated with a spherical wave which converges towards the point where the optical axis intersects the principal plane of the lens, see Fig. 10.

iii. The phase of the quadratic phase term changes by an amount which is only a fraction of a radian within the object region which contributes significantly to a particular image point. This statement is valid if the object is not greater than a quarter of the size of the lens aperture.

The recorded intensity of the interfering spherical reference wave, shown in Eq. 20, and the object wave is:

$$I = u\left(\frac{x'}{M}\right)^2 + A_r^2 + 2u\left(\frac{x'}{M}\right) A_r \cos\left[\frac{\pi}{\lambda}\left(\frac{x'^2}{d_2} - \frac{x'^2}{d_r} + 2\frac{x'x_r}{d_r} - \frac{x_r^2}{d_r}\right)\right] \tag{38}$$

Assuming ($d_r = d_2$), substituting $x_r = \lambda d_r \nu_r$ and neglecting $\left(\frac{\pi x_r^2}{\lambda d_r}\right)$, which only introduces a constant phase offset, results in:

$$I = u\left(\frac{x'}{M}\right)^2 + A_r^2 + 2u\left(-\frac{x'}{M}\right) A_r \cos\left(2\pi x' \nu_r\right) \tag{39}$$

From Eq. 39 can be concluded that, in an off-axis configuration, the phase adapted spherical reference wave introduces only a phase-tilt to a recorded Image-plane hologram. The three spatial frequency components encoded in the hologram can be separated by applying a Fourier-transformation to the recorded intensity.

$$(x_o, \nu_o) \rightarrow (x_o \cdot M, [-(\nu_{x'} + \nu_r), 0, (\nu_{x'} + \nu_r)]) \tag{40}$$

Although a magnification (M) is applied to the image, the SBP' and SBP'' must still be kept constant as discussed in the Introduction. The highest resolvable spatial frequency is determined by the NA of the lens.

$$\nu_{x'} = 2\frac{NA}{\lambda} = \frac{2x'}{\lambda M f} \tag{41}$$

The spatial image frequency $\nu_{x'}$ is inversely proportional to M. Although all conditions have been set to enable the correct recording of the object's intensity and phase, the resulting SBP'' of an Image-plane hologram does not automatically match the object's SBP. A lens-pupil of infinite extent was assumed in deriving the imaging equation. In practice the lens is spatially limited by its aperture of diameter D. The ideal image resulting from $u'(x')$ is convolved with the Fraunhofer diffraction pattern of the lens-aperture $P(\tilde{x})$. Thus, the lens-aperture acts as a low-pass filter which stops the transition of any spatial frequency higher than the NA of the aperture allows for, see Eq. 42. The spatial frequency bandwidth of the lens $\Delta\nu_L$ can be described as:

$$|\nu(x')| \leq \Delta\nu_L = 2\frac{\mathrm{NA}}{\lambda} = 2\frac{n \sin\left[\arctan(\frac{D}{2f})\right]}{\lambda} \approx \frac{D}{\lambda f} \tag{42}$$

Furthermore, the spatial frequency bandwidth $\Delta\nu_{x'}$ decreases the more out-of-field the object point is located. This effect is due to lens aberrations, which increase the more laterally displaced from the optical axis the object point is located, as shown in Fig. 11. Hence Eq. 42 is strictly speaking only applicable for small objects in close proximity to the optical axis.

In-line Setup

SBP′ for an in-line configuration is therefore defined by the lens parameters:

$$\boxed{SBP'_{in-line} = D\Delta\nu_L = X_L\Delta\nu_L = SBP_L} \tag{43}$$

Off-axis Setup

The separation of the image, twin-image and DC term is obtained by choosing the inclination angle of the reference wave to be larger than the largest light inclination angle introduced by any imaging ray:

$$\nu_r \geq \Delta\nu_L/2 \tag{44}$$

The required SBP′ for the off-axis configuration needs to have the same spatial width as the recorded image.

$$X \geq X_L \tag{45}$$

The spatial frequency bandwidth in the hologram-plane is defined as:

$$x'\Delta\nu' = 2\nu_r + \Delta\nu_L \geq 2\Delta\nu_L \tag{46}$$

Thus the required SBP′ for the digital sensor is:

$$\boxed{SBP_{off-axis} \geq 2X_L\Delta\nu_L = 2SBP_L} \tag{47}$$

The in-line and off-axis SBP for an Image-plane hologram are shown in Fig. 11.

3. SBP″ or Performance Capacity

The SBP″ of the reconstructed hologram is described by the product of the reconstructed FOV, which is represented in one-dimension by X'' and the spatial frequency bandwidth, which is the reciprocal value of the smallest resolvable object detail $\delta_{x''}$ (see Eq. 2).

$$SBP'' = X'' \cdot \frac{1}{\delta_{x''}} \tag{48}$$

A. Fresnel hologram

In the first case the recording of a Fresnel hologram is considered. The minimum recording distance differs according to an in-line or off-axis configuration and can be derived from the phase term represented in Eq. 10, in which the continuously defined coordinates are replaced by their numerical counterparts ($x' = k\Delta x'$, where k is the position counter and $\Delta x'$ the pixel-size). The largest recorded spatial frequency results from the interference of the reference wave and furthest distant object point $\left(x = -\frac{X}{2}\right)$ (see Fig. 3). Furthermore, a single object point source is assumed ($\nu_o = 0$), which results in a phase of:

$$\varphi = 2\pi k\Delta x'\nu_r + \frac{\pi}{\lambda d}\left(k\Delta x' + \frac{X}{2}\right)^2 \tag{49}$$

According to Nyquist's criterion the phase difference between two adjacent pixels, which depends on the pixel position k within the sensor matrix, should not exceed π. Therefore, Eq. 49 needs to be differentiated with respect to k.

$$\frac{\Delta\varphi}{\Delta k} \approx \frac{\partial\varphi}{\partial k} = 2\pi\Delta x'\nu_r + \frac{2\pi}{\lambda d}\left(k\Delta x' + \frac{X}{2}\right)\Delta x' \tag{50}$$

The highest spatial frequency is recorded at the edge of the detector $\left(k = \frac{N}{2}\right)$, with $\Delta k = 1$. Both values are then substituted in Eq. 50.

$$\pi \geq \left|2\pi\Delta x'\nu_r + \frac{\pi}{\lambda d}\left(N\Delta x' + X\right)\Delta x'\right|, \text{ where } N \text{ is the pixel number} \tag{51}$$

Assuming an in-line setup ($\nu_r = o$) and solving Eq. 51 for the distance results in:

$$d_{in-line} = \frac{(X + N\Delta x')\Delta x'}{\lambda} \tag{52}$$

In the off-axis configuration the reference frequency introduced by the inclination angle α should be large enough to separate the various imaging terms in the Fourier domain. It is assumed that the DC terms have numerically been suppressed by one of the method described in [8] and in [10], which results in:

$$\nu_r = \frac{\alpha}{\lambda} = \frac{X}{\lambda d} \tag{53}$$

Substituted in Eq. 51 results in:

$$d_{off-axis} = \frac{(3X + N\Delta x')\Delta x'}{\lambda} \tag{54}$$

Not having suppressed the DC term would have resulted in more than twice the recording distance $\left(d_{off-axis} = \frac{(7X+N\Delta x')\Delta x'}{\lambda}\right)$, by which the optical resolution obtained would significantly have been reduced. The one dimensional FOV for both cases can be obtained by rearranging Eqs. 52 and 54 for the object-size X:

$$X_{in-line} = \frac{d\lambda}{\Delta x'} - N\Delta x' \tag{55}$$

$$X_{off-axis} = \frac{d\lambda - N\Delta x'^2}{3\Delta x'} \tag{56}$$

The smallest resolvable object detail is a function of the holographic system's (NA), which is determined by the recording distance and the sensor size.

$$\frac{1}{\Delta\nu(x'')} = \delta(x'') = \frac{\lambda d}{N\Delta x'} \tag{57}$$

Replacing d with $d_{in-line}$ and $d_{off-axis}$ results in:

$$\frac{1}{\Delta\nu(x'')_{in-line}} = \delta(x'')_{in-line} = \frac{X + N\Delta x'}{N} \tag{58}$$

$$\frac{1}{\Delta\nu(x'')_{off-axis}} = \delta(x'')_{off-axis} = \frac{3X + N\Delta x')}{N} \tag{59}$$

The obtained SBP'' can be described as a function of either the object size X or the recording distance d:

$$\boxed{\begin{aligned} SBP''_{in-line} &= \frac{X \cdot N}{X + N\Delta x'} = N - \frac{(N\Delta x')^2}{d\lambda} \\ SBP''_{off-axis} &= \frac{X \cdot N}{3X + N\Delta x'} = \frac{1}{3}\left(N - \frac{(N\Delta x')^2}{d\lambda}\right) = \frac{1}{3} \cdot SBP''_{in-line} \end{aligned}} \tag{60}$$

B. Fourier hologram

The plane reference wave has been replaced by a divergent *spherical reference wave*. Both points, object and source, of the spherical reference wave are positioned at the same distance to the camera. This results in an equal curvature of reference and object-waves. Thus the interference fringes are homogenously distributed across the sensor. The minimum recording distance for in-line and off-axis can be derived from Eq. 22 in a similar manner to that used for the investigation of Fresnel holograms.

$$\begin{aligned} \varphi &= \frac{\pi}{\lambda d}\left(-2x'x_o + x_o^2 + 2x'x_r - x_r\right) \\ \varphi &= \frac{\pi}{\lambda d}\left(-2k\Delta x'x_o + x_o^2 + 2k\Delta x'x_r - x_r\right) \end{aligned} \tag{61}$$

Differentiating Eq. 61 with respect to k and applying Nyquist's criterion results in the following inequality:

$$\pi \geq \left|2\Delta x'\Delta k\frac{\pi}{\lambda d}\left(-x_o + x_r\right)\right| \tag{62}$$

The minimum recording distance for an in-line setup is obtained by replacing the following parameters with the following values $x_o = X/2$ (see Fig. 7), $x_r = 0$ and $\Delta k = 1$:

$$d_{in-line} = \frac{X\Delta x'}{\lambda} \tag{63}$$

The minimum distance for an off-axis setup with $x_r = -X/2$ (see Fig. 7) is:

$$d_{off-axis} = \frac{2X\Delta x'}{\lambda} \tag{64}$$

The corresponding FOV for in-line and off-axis arrangement are:

$$X_{in-line} = \frac{d\lambda}{\Delta x'} \tag{65}$$

$$X_{off-axis} = \frac{d\lambda}{2\Delta x'} \tag{66}$$

Consequently the SBP''s for in-line and off-axis configurations are:

$$\boxed{\begin{aligned} SBP''_{in-line} &= N \\ SBP''_{off-axis} &= \frac{N}{2} = \frac{1}{2} \cdot SBP''_{in-line} \end{aligned}} \tag{67}$$

C. Image-plane hologram

The FOV for an Image-plane hologram is:

$$X = \frac{N\Delta x'}{M} = \frac{N\Delta x' f}{d_2 - f} \tag{68}$$

The highest recordable spatial object frequency depends on the NA of the lens-system with respect to Rayleigh's criterion.

$$|\nu(x'')| = \nu(x') = \frac{D}{1.22\lambda f}$$

Thus the SBP'' becomes:

$$\boxed{SBP'' = \frac{N\Delta x' f}{d_2 - f}\left(\frac{D}{1.22\lambda f}\right)} \tag{69}$$

4. Discussion and Conclusion

The required SBP' in the recording process and SBP'' in the reconstruction process for Fresnel holograms, Fourier holograms and Image-plane holograms were derived. The best performance for SBP' and SBP'' is obtained by utilizing a lens-less Fourier hologram. The SBP performance of the Image-plane hologram depends to a high degree on the lens-system employed. Due to the following advantages of a lens-less setup the introduction of a lens system should be avoided unless the object is either too small or too large to be directly recorded with a lens-less setup:

i. The spatial cutoff frequency ν_{cutoff} for a rectangular aperture, as represented by most digital sensors, is larger than for a circular aperture, as shown in [15].

ii. The fringe contrast obtained for various spatial frequencies is larger for a rectangular aperture.

iii. Small inhomogeneities in the pixel response have a reduced influence on the image-quality than for image-plane holograms. This is due to the fact that the object information is not localized in a single point only.

iv. In lens-less holography all object points are recorded with approximately the same dynamic range. An Image-plane hologram displays sharp features such as edges with a higher grey level value, which decreases the dynamic range for other object information.

Another important difference between the recording of lens-less holograms and Image-plane holograms is that the smallest resolvable object detail δ in lens-less holography is determined by the sensor-size X'. In contrast, for an Image-plane hologram the smallest resolvable object detail δ is determined by the pixel-size $\Delta x'$ in conjunction with the NA of the lens-system. On the other hand the size of the recordable object depends on the pixel-size $\Delta x'$ for lens-less holography, whereas in image-plane holography it depends on the sensor-size X' and the parameters of the lens-system. In addition, a *Fourier hologram* when compared to a Fresnel hologram, benefits from:

1. Mathematical simplicity which reduces the computational effort when numerically reconstructing the hologram.

2. The reconstruction of the modulus by means of a two dimensional Fourier-transformation is not restricted to a minimum distance, whereas the reconstruction of a Fresnel-hologram utilizing the Fresnel-method is only valid within the Fresnel regime.

3. Reduced recording distance compared to Fresnel-holograms, which results in an increased optical resolution.

4. No need to introduce lenses between reference wave point source and object. A Fresnel hologram instead requires lenses for the collimation of the reference beam. In this manner costs, disturbing diffraction effects from dust on optical surfaces and wave-aberrations introduced in the collimation process are minimized.

6. Low coherence light sources can be used in conjunction with the investigation of microscopic objects, since matched reference and object wave curvature requires less temporal coherence. This results in reduced speckle-noise and improved image quality.

7. Reduced risk for recording an undersampled hologram, since the fringe density is almost homogeneous across the entire hologram. An undersampled Fourier hologram would result in an unsuccessful reconstruction, since the interference fringes cannot be recorded by the sensor.

In conclusion, it could be shown that the SBP is an important tool to compare and investigate different holographic systems in terms of their required sensor specification and reconstruction capacity. The knowledge obtained can be applied to the setup of a holographic system which is best adapted to the object's SBP.

References

1. A. W. Lohmann. The space-bandwidth product, applied to spatial filtering and to holography. *IBM Research Paper*, RJ-438, 1967.
2. L. Xu, Z. Guo X. Peng, J. Miao, and A. Asundi. Imaging analysis of digital holography. *Opt. Express*, 13(7):2444–2552, 2005.
3. J. W. Goodman. *Introduction to Fourier Optics*. McGraw-Hill, second edition edition, 1996.
4. F. Dubois, C. Schockaert, N. Callens, and C. Yourassowsky. Focus plane detection criteria in digital holography microscopy by amplitude analysis. *Opt. Express*, 14(13):5859–5958, 2006.
5. D. P. Kelly, B. M. Hennelly, C. McElhinney, and T. J. Naughton. A practical guide to digital holography and generalized sampling. *Proc. SPIE*, 7072:707215, 2008.
6. A. W. Lohmann, M. E. Testorf, and J. Ojeda-Castañeda. *The art and science of holography: a tribute to Emmett Leith and Yuri Denisyuk*, chapter Holography and the Wigner function. SPIE Press, 2004.
7. U. Schnars and W. Jueptner. *Digital Holography*. Springer, 2005.
8. T. Kreis. *Handbook of holographic interferometry: optical and digital methods*. Wiley-VCH, 2005.
9. L. Z. Cai, Q. Liu, and X. L. Yang. Generalized phase-shifting interferometry with arbitrary unknown phase steps for diffraction objects. *Opt. Lett.*, 29(2):183–185, 2004.
10. U. Schnars. *Digtal Holography*. Springer, 2005.
11. P. Hariharan. *Optical holography*. Cambridge University Press, 1984.
12. A. W. Lohmann and S. Sinzinger. *Optical Information Processing*. Universitätsverlag Ilmenau, 2006.
13. E. Zeidler, H. R. Schwarz, and W. Hackbusch. *Taschenbuch der Mathematik*. B.G.Teubner, 1996.
14. R. Bracewell. *The Fourier Transform and Its Applications*, chapter The Impulse Symbol, pages 69–97. McGraw-Hill, 1986.
15. G. O. Reynolds, J. B. DeVelis, G. B. Parrent, and B. J. Thompson. *The new physical optics notebook: tutorials in fourier optics*. SPIE Press, 1989.
16. A. W. Lohmann. Space-bandwidth product of optical signals and systems. *J. Opt. Soc. Am. A*, 13(3):470–473, 1996.

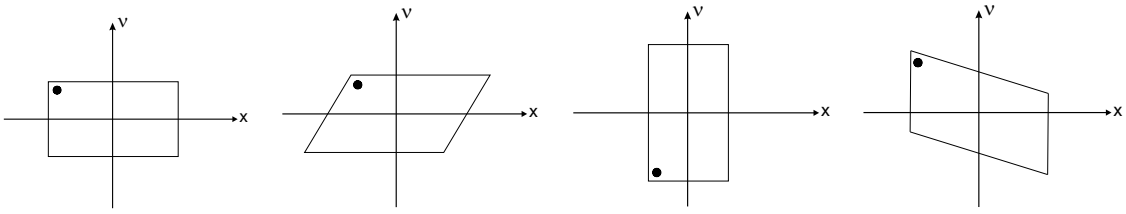

(a) (b) (c) (d)

Fig. 1. Adopted Figs. taken from [16] (a) SBP in the space-frequency domain, (b) SBP of (a) after Fresnel transformation, (c) SBP of (a) after Fourier transformation, (d) SBP of (a) after passage through lens

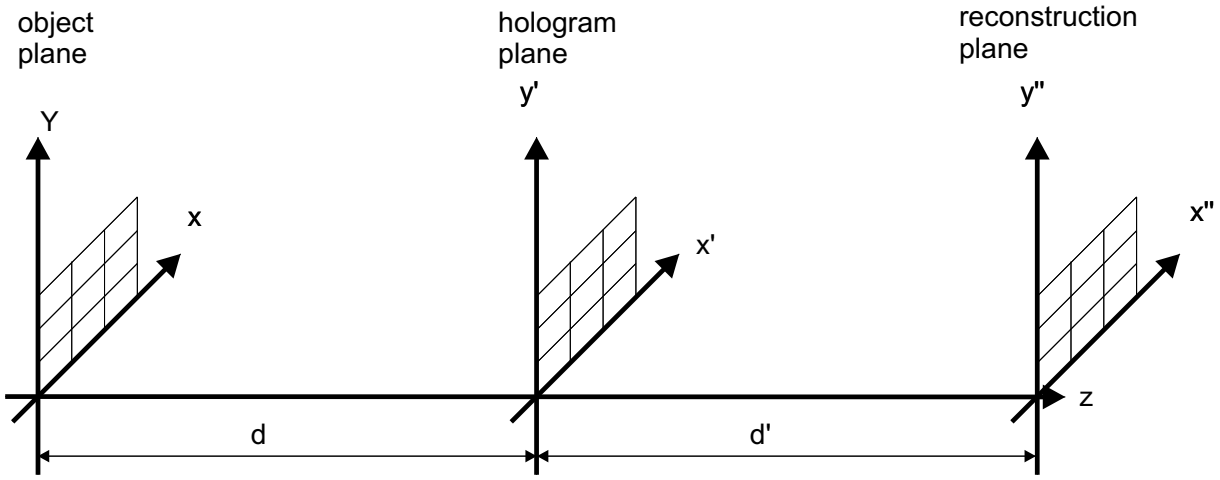

Fig. 2. Nomenclature of coordinates used for the holographic recording and reconstruction process

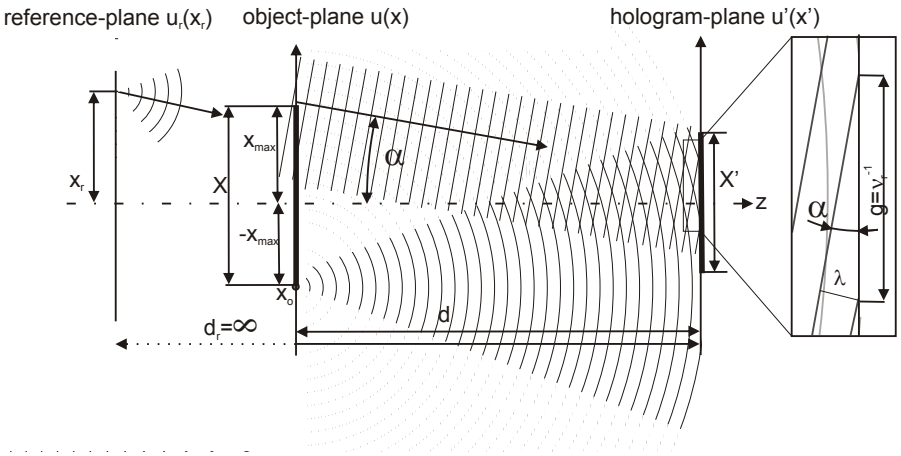

Fig. 3. Carrier frequency introduced by inclination of plane reference wave

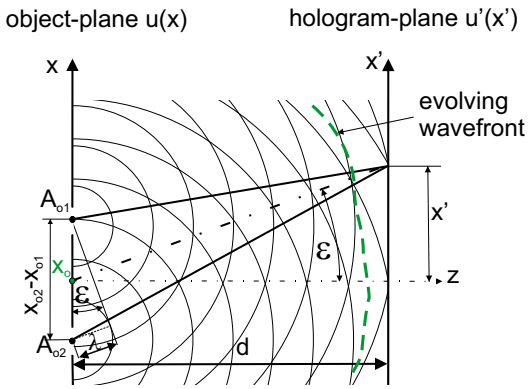

Fig. 4. (Color online) Interference pattern caused by smallest resolvable object detail

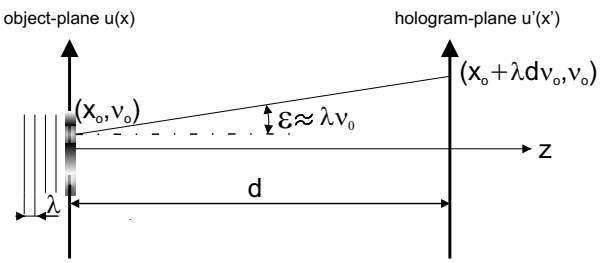

Fig. 5. Diffracted cone of light from object coordinate x_o to hologram-plane

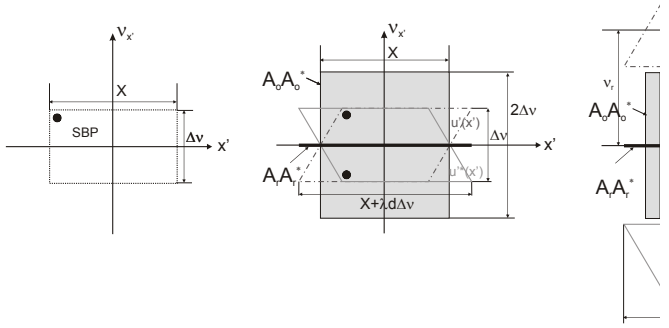

(a) (b) (c) (d)

Fig. 6. Fresnel-hologram, (a) original SBP of object, (b) SBP′ in-line, (c) SBP′ off-axis without suppression of DC term, (d) SBP′ off-axis with suppression of DC term

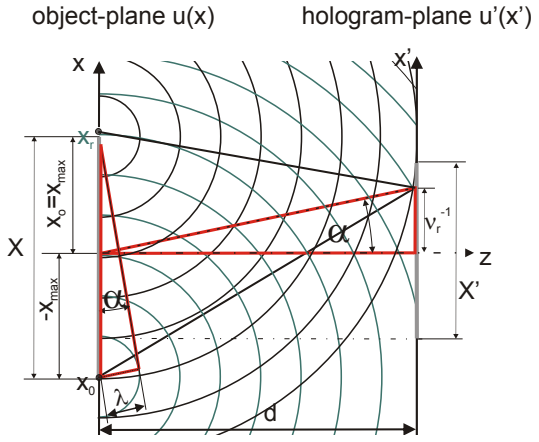

Fig. 7. (Color online) Carrier frequency introduced by a lateral displacement of the origin of the spherical reference wave

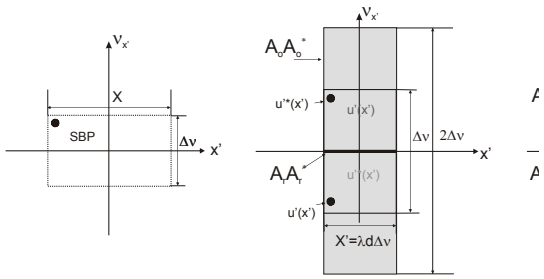

(a) (b) (c) (d)

Fig. 8. Fourier-hologram, (a) original SBP of object, (b) SBP′ in-line, (c) SBP′ off-axis without suppression of DC term, (d) SBP′ off-axis with suppression of DC term

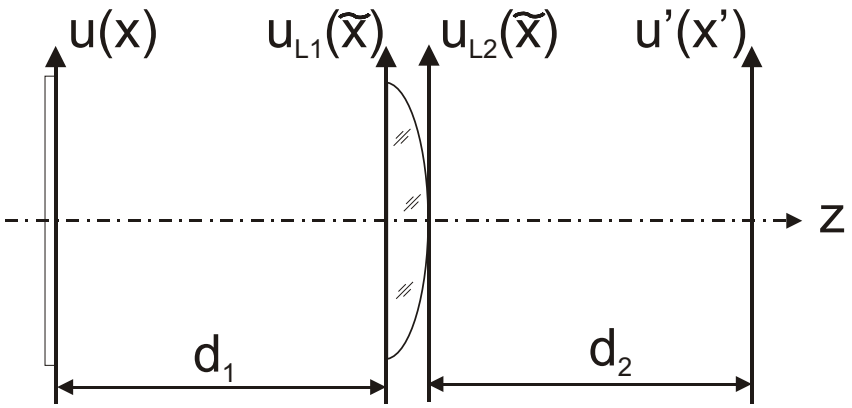

Fig. 9. Sketch of different planes involved in the image formation

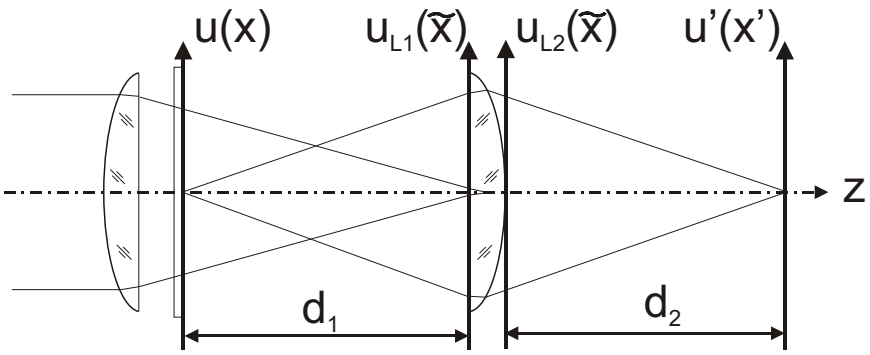

Fig. 10. Convergent object illumination to suppress quadratic phase term

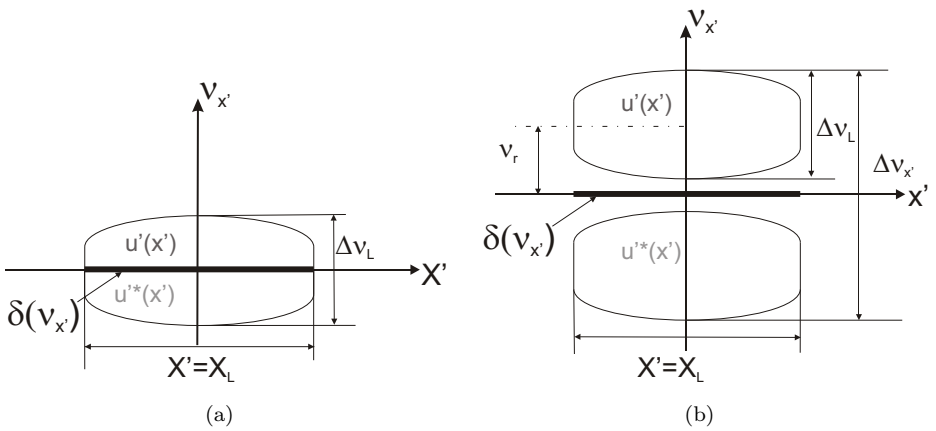

Fig. 11. SBP of an Image-plane hologram, (a) in-line arrangement, (b) off-axis arrangement